This article has been accepted for publication in a future issue of this journal, but has not been fully edited. Content may change prior to final publication. Citation information: DOI 10.1109/LAWP.2021.3095394, IEEE Antennas and Wireless Propagation Letters

Two-Row ESPAR Antenna with Simple Elevation and Azimuth Beam Switching

M. Rzymowski, *Member, IEEE* and L. Kulas, *Senior Member, IEEE*

***Abstract*—In this letter, we propose a two-row electronically steerable parasitic array radiator (ESPAR) antenna designed for direction of arrival (DoA) estimation in Internet of Things (IoT) applications relying on simple microcontrollers. The antenna is capable of elevation and azimuth beam switching using a simple microcontroller-oriented steering circuit, and provides 18 directional radiation patterns, which can be grouped in 3 distinctive sets having different directions in the elevation. For each elevation direction, there are 6 different beam configurations that cover 360 degrees in the horizontal plane. Measurements of the realized antenna prototype carried out in an anechoic chamber show good agreement with numerical simulations. The antenna prototype provides low side lobe level (SLL), low half power beam width (HPBW) in both elevation and horizontal directions, and exhibit monotonous drop from the maximum value for all 18 radiation patterns. Therefore, the antenna is a good candidate for IoT nodes capable of DoA estimation in situations when radio frequency (RF) signals are impinging the antenna from different directions in elevation.**

***Index Terms*—Switched-beam antenna, electronically steerable parasitic array radiator (ESPAR) antenna, direction-of-arrival (DoA), received signal strength (RSS), wireless sensor network (WSN), internet of things (IoT).**

I. Introduction

In many modern Internet of Things (IoT) applications, information about position of IoT nodes or direction of received radio frequency (RF) signals is required to improve the network operation with respect to a number of aspects such as energy-efficiency, connectivity, security and privacy [1]-[4]. The increasing number of applications requires localization of objects that are moving or are located on different heights and distances within the same area. The most practical and relevant examples include industrial sites [5], [6] and drone applications [7], [8], in which the relative height between a localized object and a base station may vary. For this reason, dedicated reconfigurable antenna systems are being developed and integrated within final applications [5], [7], [9], [10]. The main requirements with regard to these solutions are to provide the highest possible direction of arrival (DoA) estimation accuracy, while keeping energy consumption and total costs, which are related to fabrication, deployment, and system maintenance, at the minimal level.

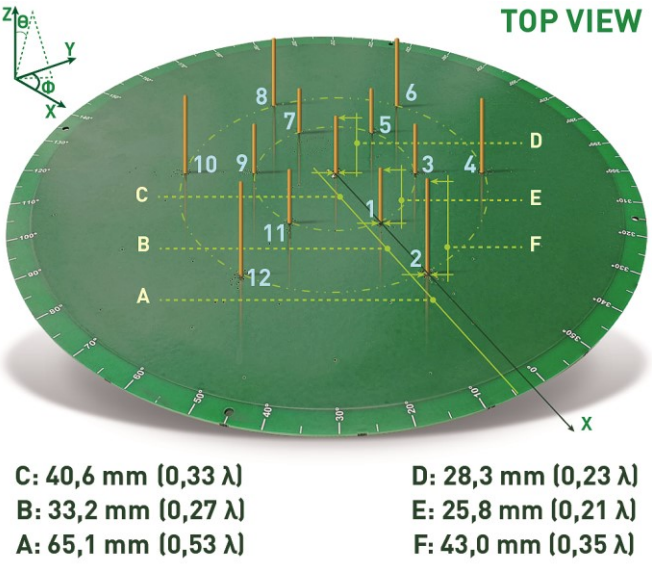

Fig. 1. Designed and realized two-row ESPAR antenna prototype together with its dimensions and numbering of its passive elements.

One of the most promising reconfigurable antenna concepts that can be integrated with a simple low-cost wireless sensor network (WSN) node is electronically steerable parasitic array radiator (ESPAR) antenna originally proposed in [11]. Such antennas have a number of passive elements, which are connected to electronically steerable reactances, surrounding a single active element in the center. Therefore, by setting the reactances to specific values, low-cost and energy-efficient realizations of ESPAR antennas can provide electronic beam steering capability for currently available on the market commercial off-the-shelf (COTS) transceivers, which have only a single RF chain, to create a WSN node with DoA estimation capability [9].

In the available literature, there is a number of DoA estimation experiments conducted with ESPAR antennas [9], [11]-[14] showing that it possible to obtain a single degree accuracy during DoA estimation when all considered RF signals are coming from the horizontal plane (i.e. θ = 90°).

This paper is a result of the InSecTT project which has received funding from the ECSEL Joint Undertaking (JU) under grant agreement No 876038. The JU receives support from the European Union's Horizon 2020 research and innovation programme and Austria, Sweden, Spain, Italy, France, Portugal, Ireland, Finland, Slovenia, Poland, Netherlands, Turkey". The document reflects only the authors' view and the Commission is not responsible for any use that may be made of the information it contains. The authors are with the Department of Microwave and Antenna Engineering, Faculty of Electronics, Telecommunications and Informatics, Gdansk University of Technology, Narutowicza 11/12, 80-233 Gdansk, Poland (corresponding author: mateusz.rzymowski@pg.edu.pl).

This work is licensed under a Creative Commons Attribution 4.0 License. For more information, see https://creativecommons.org/licenses/by/4.0/

This article has been accepted for publication in a future issue of this journal, but has not been fully edited. Content may change prior to final publication. Citation information: DOI 10.1109/LAWP.2021.3095394, IEEE Antennas and Wireless Propagation Letters

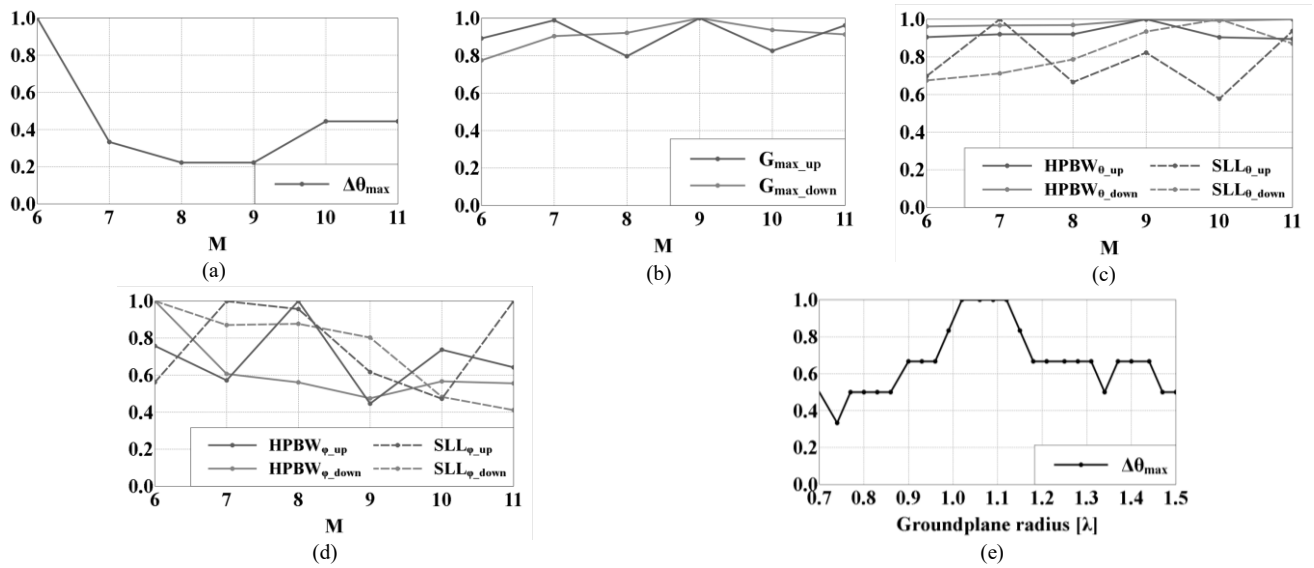

Fig. 2. Normalized antenna parameters in function of array elements (a) – (d) and groundplane radius (e) (see text for explanations): (a) maximum angular separation between radiation patterns in elevation, (b) antenna maximal gain, (c) HPBW and SLL in elevation, (d) HPBW and SLL in azimuth, (e) maximum angular separation between radiation patterns in elevation in function of groundplane radius.

However, when different elevation angles of incoming RF signals impinging the antenna are considered, DoA estimation accuracy deteriorates for low θ angles [15]-[17], which is related to the conical radiation pattern of ESPAR antenna having a directional beam. In consequence, one may expect higher DoA estimation errors underneath the antenna in many practical situations, e.g. when base stations are mounted on different heights across industrial sites [5], [6] or are placed on inspection drones [7], [8], in which the relative height between a localized object and a base station may dynamically change.

To increase DoA estimation accuracy for all elevation angles, one might introduce variable inclination of the main directional beam in the elevation plane, which can be achieved by introducing an additional row of passive elements. So far, available designs of ESPAR antennas having an additional row of passive elements provide dual-band operation [18]-[21], better radiation parameters in the horizontal plane [22] or improved connectivity [23]. However, according to the authors knowledge, such concept has never been used for beam switching in elevation in order to increase DoA estimation accuracy in situations, where incoming RF signals are impinging the antenna from different directions in the elevation plane.

In this letter, we propose ESPAR antenna with additional row of switched parasitic elements for the radiation pattern steering in the elevation plane. The antenna was designed in such a way that all available directional radiation patterns have low side lobe level (SLL), low half power beam width (HPBW) in both elevation and horizontal directions, and exhibit monotonous drop from their maximum value, which is crucial to provide DoA estimation with high accuracy [24]. The realized antenna prototype has 18 different configurations of its radiation patterns, which can be grouped in 3 distinctive sets having different directions in the elevation. For each elevation direction, 6 directional beam configurations in the horizontal plane are possible, which was proven to reduce complexity and cost of the switching circuit [25] together with time necessary for the DoA estimation process [16] without a critical impact on the overall DoA estimation accuracy in the horizontal direction [16], [25].

II. Antenna Design

In the proposed antenna concept shown in Fig. 1, the centrally located quarter-wave active monopole is surrounded by $N = 12$ passive elements equally arranged in two circular rows, each containing $M = N/2 = 6$ passive elements. All elements are located on the metal groundplane realized as a top layer of a dielectric substrate. The active element in the middle is fed by an RF signal, while the neighbouring passive elements can be opened or shorted to the ground by low-current single-pole double-throw (SPDT) switches. In ESPAR antennas, beam steering is realized by proper configuration of the passive elements that in case of being shorted to the ground become reflectors and when opened act as directors [26], [9], [11]. Therefore directional radiation patterns can be configured digitally by a simple external microcontroller connected to the SPDT switches. In consequence, every radiation pattern can be associated to a steering vector $V = [v_1, v_2, \dots, v_s, \dots, v_{12}]$, in which v_s denotes the state of the sth passive element: v_s=1 for opened passive element, and v_s=0 is for the shortened one.

During the first step of the design process, a simplified antenna model was created in EM FEKO simulation environment for center frequency 2.44 GHz to verify all possible configurations of passive elements and to find two similar directional beams with different inclination angle. It was assumed that at least two distinctive sets of directional radiation patterns having different main beam inclination to the antenna groundplane can be created using two-row ESPAR antenna. Therefore, in this design step, the antenna was optimized to achieve the highest possible difference in the elevation

MOST WIEDZY Downloaded from mostwiedzy.pl

This work is licensed under a Creative Commons Attribution 4.0 License. For more information, see https://creativecommons.org/licenses/by/4.0/

This article has been accepted for publication in a future issue of this journal, but has not been fully edited. Content may change prior to final publication. Citation information: DOI 10.1109/LAWP.2021.3095394, IEEE Antennas and Wireless Propagation Letters

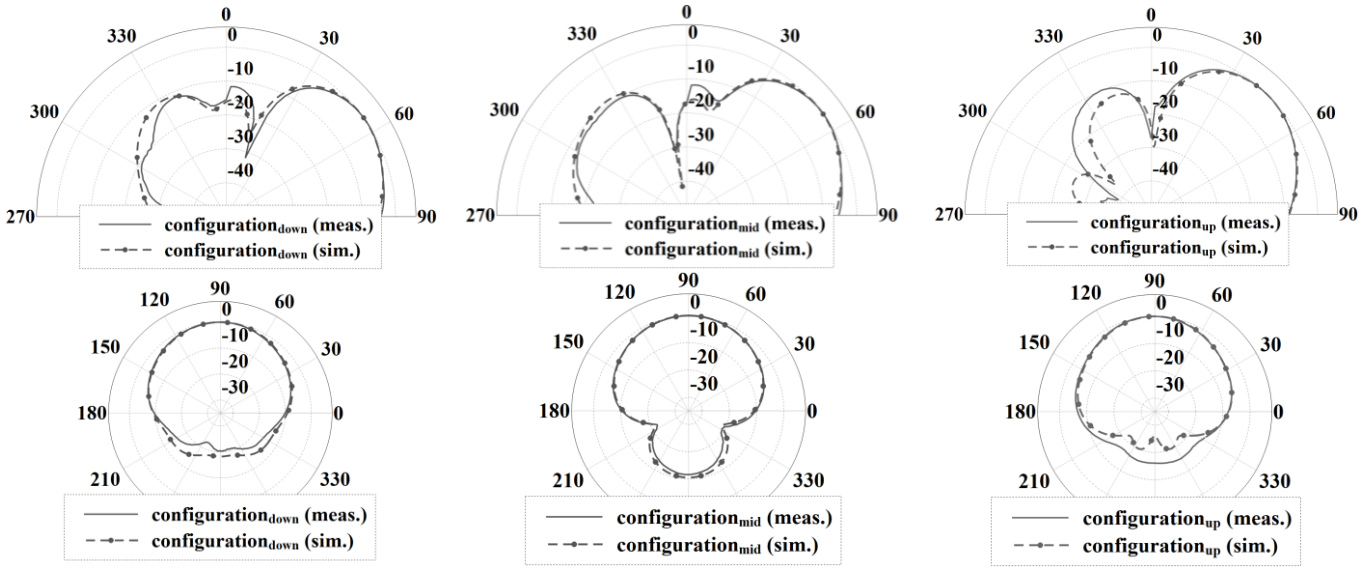

(a) (b) (c)

Fig. 3. Simulated and measured antenna radiation patterns at 2.44 GHz in the elevation plane (for φ = 0) and in the horizontal plane for three configurations (see text for explanations): (a) $V^1_{conf\_down} = [101000010010]$ (maximum at $\theta_{max\_down} = 56°$), (b) $V^1_{conf\_mid} = [010000100000]$ (maximum at $\theta_{max\_mid} = 52°$), and (c) $V^1_{conf\_up} = [110100010001]$ (maximum at $\theta_{max\_up} = 46°$).

direction between radiation patterns that can be expressed as:

$$max(\Delta\theta_{max}) = max\left(\left|\theta_{max\_up} - \theta_{max\_down}\right|\right) \quad (1)$$

where θ_{max_down} and θ_{max_up} are directions of the main beam in elevation corresponding to 2 steering vector configurations, for which the antenna directional radiation patterns reach their maximum values in elevation and have the same direction in azimuth. In parallel, additional optimization goals were set to maximize the directivity for both configurations and to minimize their SLLs. Moreover, for every optimization run the number of elements in the both rows was set to a specific value $M \in \langle 6,11 \rangle$ to verify how the total number of passive elements $N = 2M$ have influenced $\Delta\theta_{max}$ and key radiation pattern parameters. The initial optimizations were performed with a combination of grid search method to find the proper configuration of switches and genetic algorithm to achieve the expected radiation parameters. Values less than $M = 6$ have not been examined due to the insufficient discrete angular step in azimuth that could affect the DoA estimation accuracy in the horizontal direction [16], [25].

The results presented in Fig. 2 show that selection of the total number of elements is a compromise between the maximum tilt in elevation, radiation patterns parameters, structure complexity, which grows with N, and discrete angular step in the horizontal plane equal $360°/M$. The radiation pattern is improved in the horizontal plane for higher N but at the expense of angular separation in elevation $\Delta\theta_{max}$, which is one of the main criteria of the project. It can also be seen that the impact of the number of the passive elements on HPBW and SLL values is significantly lower in case of the elevation plane (Fig.2c) then in the horizontal one (Fig.2d).

Taking the above into account, $M = 6$ has been chosen as the optimal value with respect to the design goals, and then the influence of the ground plane radius on $\Delta\theta_{max}$ has additionally been investigated. The results presented in Fig. 2e show that the groundplane size has a direct influence on the angular separation in elevation $\Delta\theta_{max}$, which reaches the highest value when the groundplane radius is around λ.

In the final step, the antenna was fine-tuned with global response surface method (GRSM) to find the additional configuration, for which a set of 6 antenna directional radiation patterns reach the maximum value in elevation for θ_{max_mid} that is a θ angle fulfilling the condition that $\theta_{max\_down} < \theta_{max\_mid} < \theta_{max\_up}$. To this end, a detailed full-wave 3D antenna model involving 1.55mm height FR4 laminate with metalized top layer with proper loads extracted from available S parameters of NJG1681MD7 SPDT switches, which were used as switching circuits located on the bottom layer of PCB, has been realized and tuned with respect to the abovementioned optimization goals. In consequence, numerical results produced in EM FEKO simulation environment for the final antenna design indicate that it has been possible to get three different radiation patterns sets having $\theta_{max\_down} = 56°$, $\theta_{max\_mid} = 52°$, and $\theta_{max\_up} = 46°$ obtained for $V^1_{conf\_down} = [101000010010]$, $V^1_{conf\_mid} = [010000100000]$, and $V^1_{conf\_up} = [110100010001]$ respectively. Moreover, by applying circular shift to these vectors, it is possible to rotate each beam in the horizontal plane by 360° with a discrete angular step of 60°.

III. Realization and Measurements

To verify the simulation model, the antenna has been fabricated and measured. The realized antenna is presented in Fig. 1. It has been realized on 1.55mm height FR4 laminate with metalized top layer. The switching circuits realized with NJG1681MD7 SPDT switches are located on the bottom layer of PCB underneath each of the passive elements as shown in Fig. 4. The proposed switching circuits have been chosen due

MOST WIEDZY Downloaded from mostwiedzy.pl

This work is licensed under a Creative Commons Attribution 4.0 License. For more information, see https://creativecommons.org/licenses/by/4.0/

This article has been accepted for publication in a future issue of this journal, but has not been fully edited. Content may change prior to final publication. Citation information: DOI 10.1109/LAWP.2021.3095394, IEEE Antennas and Wireless Propagation Letters

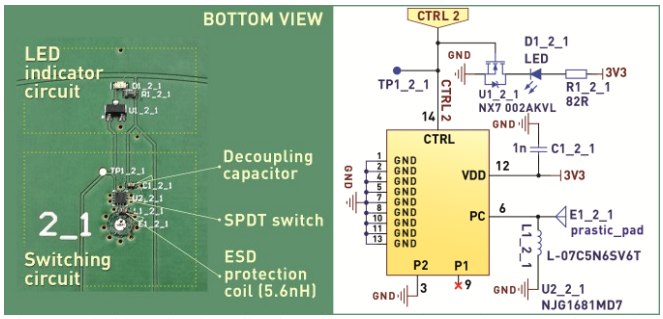

Fig. 4. Switching circuit realized on the antenna bottom layer together with its corresponding schematic layout.

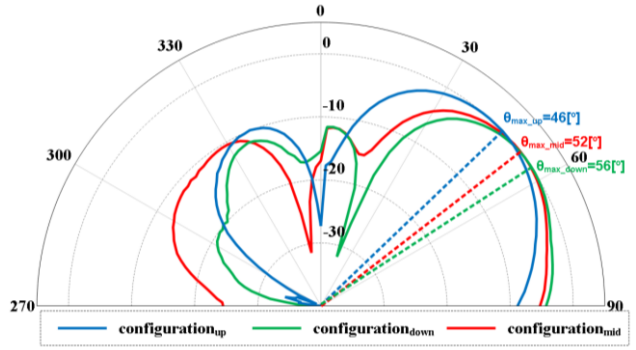

Fig. 5. Antenna radiation patterns measured at f=2.44 GHz in the elevation plane (for φ=0) for all three considered configurations: $V^1_{conf\_down}$, $V^1_{conf\_mid}$, and $V^1_{conf\_up}$ (see text for explanations).

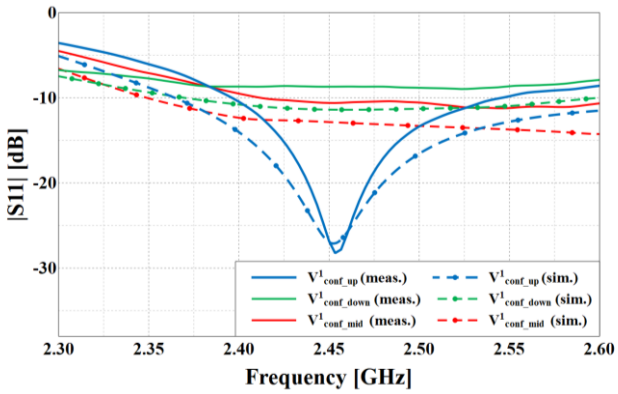

Fig. 6. Values of |S11| for all three considered configurations: $V^1_{conf\_down}$, $V^1_{conf\_mid}$, and $V^1_{conf\_up}$ (see text for explanations).

to low insertion losses, high isolation and low energy consumption when comparing to PIN diodes or other switches available on the market. They are powered and steered via an external controller with 3.3V voltage. To indicate the actual state of the switch, a dedicated LED indicator circuit has been introduced. The diode emits light when the steering signal is high and the circuit is in the open state. A decoupling capacitor and ESD protection coil have been located close to the switch to guarantee its proper operation. The antenna has been measured in the anechoic chamber and the resulting radiation patterns are presented in Fig. 3 and Fig. 5, while the associated numerical values are gathered in Table I.

The realized antenna provides three groups of radiation patterns that can be switched in order to point three different

TABLE I
TWO-ROW ESPAR ANTENNA PROTOTYPE PARAMETERS MEASURED AT F=2.44 GHZ

Config.	θ_{max} [°]	$HPBW_\theta$ [°]	$HPBW_\varphi$ [°]	SLL_θ [dB]	$\lvert S_{11}\rvert$ [dB]	G_{max} [dB]
up	46	45	88	10	20.9	7.7
down	56	46	93	12	8.8	8.1
mid	52	43	100	10	10.5	7.8

elevation directions with the maximum angular separation $\Delta\theta_{max} = 10°$ between them (see Fig. 3 and Fig. 5). The |S11| simulation and measurement results for all three configurations, which are presented in Fig. 6, show that achieving reasonable impedance matching for all configurations is feasible. The values of SLL, HPBW in both directions, maximal gain and S11 presented in Table I are similar for all the considered configurations and well aligned with the initial design goals and the overall assumptions. The observed differences between simulated and measured results in Fig. 3 are not significant with respect to the main direction angle values for each configuration and beamwidth in the both planes. Some discrepancies related to sidelobe levels (SLL) in elevation and backward radiation have been noticed and it has been assumed that they are caused by the imperfect switching circuits model used in the simulation and non-ideal antenna realization with respect to the passive rods.

IV. CONCLUSIONS

In this letter, an ESPAR antenna with two rows of passive elements for simple elevation and azimuth beam switching has been proposed. Different configurations have been examined and analyzed to achieve the most optimal design for future DoA applications. The final antenna prototype, measured in an anechoic chamber, has 18 different configurations that can be grouped in 3 distinctive sets having directional radiation patterns with different inclination in the elevation plane to provide 10° switching range in the elevation, which has not been earlier achieved for this kind of antenna. Moreover, every radiation pattern having the maximum at $\theta_{max\_down} = 56°$, $\theta_{max\_mid} = 52°$ or $\theta_{max\_up} = 46°$ can be switched by 360° in the azimuth with 60° discrete step to provide 6 directional beam configurations in the horizontal plane. As each of the radiation patterns has low SLL, HPBW in both elevation and horizontal directions, and exhibit monotonous drop from the maximum value, the proposed antenna may be used to improve DoA estimation accuracy in the horizontal plane when impinging RF signals come from different directions in elevation. Additionally, because the antenna relies on simple switching concept that can easily be integrated with low-cost WSN nodes, the proposed two-row ESPAR antenna can also be used to improve connectivity in IoT applications.

ACKNOWLEDGEMENT

The authors would like to thank Mateusz Czelen for his support in the preparation of the antenna prototype.

The authors would like to thank the editors and the anonymous reviewers for valuable comments that helped the authors to improve the overall quality of the article.

MOST WIEDZY Downloaded from mostwiedzy.pl

This work is licensed under a Creative Commons Attribution 4.0 License. For more information, see https://creativecommons.org/licenses/by/4.0/

This article has been accepted for publication in a future issue of this journal, but has not been fully edited. Content may change prior to final publication. Citation information: DOI 10.1109/LAWP.2021.3095394, IEEE Antennas and Wireless Propagation Letters

REFERENCES

[1] M. Tarkowski, M. Rzymowski, L. Kulas and K. Nyka, "Improved Jamming Resistance Using Electronically Steerable Parasitic Antenna Radiator," 17th International Conference on Smart Technologies (EUROCON 2017), pp. 496-500, Jul. 2017.

[2] G. S. Brar, S. Rani, V. Chopra, R. Malhotra, H. Song and S. H. Ahmed, "Energy Efficient Direction-Based PDORP Routing Protocol for WSN," in IEEE Access, vol. 4, pp. 3182-3194, 2016. doi: 10.1109/ACCESS.2016.2576475

[3] M. Asif, S. Khan, R. Ahmad, M. Sohail and D. Singh, "Quality of Service of Routing Protocols in Wireless Sensor Networks: A Review," in IEEE Access, vol. 5, pp. 1846-1871, 2017. doi: 10.1109/ACCESS.2017.2654356

[4] J. N. Al-Karaki and A. Gawanmeh, "The Optimal Deployment, Coverage, and Connectivity Problems in Wireless Sensor Networks: Revisited," in IEEE Access, vol. 5, pp. 18051-18065, 2017.doi: 10.1109/ACCESS.2017.2740382

[5] M. Cremer, U. Dettmar, C. Hudasch, R. Kronberger, R. Lerche and A. Pervez, "Localization of Passive UHF RFID Tags Using the AoAct Transmitter Beamforming Technique," in IEEE Sensors Journal, vol. 16, no. 6, pp. 1762-1771, March15, 2016, doi: 10.1109/JSEN.2015.2503640.

[6] S. Huang, O. P. Gan, S. Jose and M. Li, "Localization for industrial warehouse storage rack using passive UHF RFID system," 2017 22nd IEEE International Conference on Emerging Technologies and Factory Automation (ETFA), Limassol, 2017, pp. 1-8, doi: 10.1109/ETFA.2017.8247643.

[7] A. Buffi, P. Nepa and R. Cioni, "SARFID on drone: Drone-based UHF-RFID tag localization," 2017 IEEE International Conference on RFID Technology & Application (RFID-TA), Warsaw, 2017, pp. 40-44, doi: 10.1109/RFID-TA.2017.8098872.

[8] Marcos T. de Oliveira, Ricardo K. Miranda, João Paulo C. L. da Costa, André L. F. de Almeida, Rafael T. de Sousa, "Low Cost Antenna Array Based Drone Tracking Device for Outdoor Environments", Wireless Communications and Mobile Computing, vol. 2019, Article ID 5437908, 14 pages, 2019. https://doi.org/10.1155/2019/5437908

[9] M. Groth, M. Rzymowski, K. Nyka and L. Kulas, "ESPAR Antenna-Based WSN Node With DoA Estimation Capability," in IEEE Access, vol. 8, pp. 91435-91447, 2020, doi: 10.1109/ACCESS.2020.2994364.

[10] F. Viani, L. Lizzi, M. Donelli, D. Pregnolato, G. Oliveri, and A. Massa, "Exploitation of parasitic smart antennas in wireless sensor networks," Journal of Electromagnetic Waves and Applications, vol. 24, no. 7, pp. 993-1003, Jan. 2010.

[11] E. Taillefer, A. Hirata and T. Ohira, "Direction-of-arrival estimation using radiation power pattern with an ESPAR antenna," in *IEEE Transactions on Antennas and Propagation*, vol. 53, no. 2, pp. 678-684, Feb. 2005, doi: 10.1109/TAP.2004.841312.

[12] M. Plotka, M. Tarkowski, K. Nyka and L. Kulas, "A novel calibration method for RSS-based DoA estimation using ESPAR antennas," *2018 22nd International Microwave and Radar Conference (MIKON)*, Poznan, 2018, pp. 65-68, doi: 10.23919/MIKON.2018.8405316.

[13] L. Kulas, " RSS-based DoA Estimation Using ESPAR Antennas and Interpolated Radiation Patterns," IEEE Antennas Wireless Propag. Lett., vol. 17, no. 1, pp. 25-28, Jan. 2018.

[14] M. Tarkowski and L. Kulas, " RSS-based DoA Estimation for ESPAR Antennas Using Support Vector Classification," IEEE Antennas Wireless Propag. Lett., vol. 18, no. 4, pp. 561-565, Apr. 2019.

[15] M. Rzymowski and L. Kulas, ``RSS-based direction-of-arrival estimation with increased accuracy for arbitrary elevation angles using ESPAR antennas," in Proc. 12th Eur. Conf. Antennas Propag. (EuCAP), London, U.K., 2018, pp. 1-4.

[16] M. Burtowy, M. Rzymowski, and L. Kulas, "Low-Profile ESPAR Antenna for RSS-Based DoA Estimation in IoT Applications," *IEEE Access*, vol. 7, pp. 17403-17411, 2019.

[17] M. Groth, L. Leszkowska and L. Kulas, "Efficient RSS-Based DoA Estimation for ESPAR Antennas Using Multiplane SDR Calibration Approach," *2018 IEEE-APS Topical Conference on Antennas and Propagation in Wireless Communications (APWC)*, Cartagena des Indias, 2018, pp. 850-853, doi: 10.1109/APWC.2018.8503740.

[18] T. Noguchi, Y. Tuji, Y. Nakane and Y. Kuwahara, "Multi-band adaptive array antenna by means of switched parasitic elements," IEEE Antennas and Propagation Society International Symposium. Digest. Held in conjunction with: USNC/CNC/URSI North American Radio Sci. Meeting (Cat. No.03CH37450), Columbus, OH, 2003, pp. 916-919 vol.3, doi: 10.1109/APS.2003.1220059.

[19] O. Shibata and T. Furuhi, "Dual-band ESPAR antenna for wireless LAN applications," 2005 IEEE Antennas and Propagation Society International Symposium, Washington, DC, 2005, pp. 605-608 vol. 2B, doi: 10.1109/APS.2005.1552084.

[20] W. J. Huang, B. H. Sun, Y. Wang, F. F. Zhang and K. He, "A high-gain dual-band ESPAR antenna with simple on/off controlling," Proceedings of the 9th International Symposium on Antennas, Propagation and EM Theory, Guangzhou, 2010, pp. 315-318, doi: 10.1109/ISAPE.2010.5696463.

[21] Haitao Liu, S. Gao, Tian Hong Loh and Fei Qin, "Low-cost intelligent antenna with low profile and broad bandwidth," in IET Microwaves, Antennas & Propagation, vol. 7, no. 5, pp. 356-364, 11 April 2013, doi: 10.1049/iet-map.2011.0398.

[22] M. Rzymowski, K. Nyka and Ł. Kulas, "Enhanced switched parasitic antenna with switched active monopoles for indoor positioning systems," 2014 20th International Conference on Microwaves, Radar and Wireless Communications (MIKON), Gdansk, 2014, pp. 1-4, doi: 10.1109/MIKON.2014.6899850.

[23] R. Milne, "A small adaptive array antenna for mobile communications," 1985 Antennas and Propagation Society International Symposium, Vancouver, Canada, 1985, pp. 797-800, doi: 10.1109/APS.1985.1149485.

[24] M. Rzymowski and L. Kulas, ``Infuence of ESPAR antenna radiation patterns shape on PPCC-based DoA estimation accuracy," in Proc. 22nd Int. Conf. Microw., Radar Wireless Commun., Poznan, Poland, May 2018, pp. 69-72.

[25] M. Tarkowski, M. Rzymowski, K. Nyka and L. Kulas, "RSS-Based DoA Estimation with ESPAR Antennas Using Reduced Number of Radiation Patterns," *2019 13th European Conference on Antennas and Propagation (EuCAP)*, Krakow, Poland, 2019, pp. 1-4.

[26] D. V. Thiel and S. L. Smith, Switched Parasitic Antennas for Cellular Communications, MA, Norwood:Artech House, 2002.

MOST WIEDZY Downloaded from mostwiedzy.pl

This work is licensed under a Creative Commons Attribution 4.0 License. For more information, see https://creativecommons.org/licenses/by/4.0/